Translational Oncology 14 (2021) 101232

Contents lists available at ScienceDirect

Translational Oncology

journal homepage: www.elsevier.com/locate/tranon

Original Research

Effective killing of cells expressing CD276 (B7-H3) by a bispecific T cell engager based on a new fully human antibody

Xianglei Liu [a,b,*], Doncho Zhelev [a], Cynthia Adams [a], Chuan Chen [a], John W Mellors [a,c], Dimiter S. Dimitrov [a,c,*]

[a] Center for Antibody Therapeutics, Division of Infectious Diseases, Department of Medicine, University of Pittsburgh Medical School, S843 Scaife Hall, 3550 Terrace Street, Pittsburgh, PA 15261, United States
[b] State Key Laboratory of Bioreactor Engineering, Shanghai Collaborative Innovation Center for Biomanufacturing, East China University of Science and Technology, Shanghai 200237, China
[c] Abound Bio, 1401 Forbes Ave, Pittsburgh, PA 15219, United States

ARTICLE INFO

Keywords:
Fully human antibody
CD276 (B7-H3)
V1/V2 domain
Bispecific T cell engager (BiTE)

ABSTRACT

The pancaner molecule CD276 (B7-H3) is an attractive target for antibody based therapy. We identified from a large (10^{11}) phage-displayed single-chain variable fragment (scFv) library, a fully human antibody, B11, which bound with high avidity (K_D=0.4 nM) to CD276. B11 specifically bound to the V1/V2 domain of CD276 and competed with the antibody 8H9 (Omburtamab). It was used to design an IgG-format bispecific T cell engager B11-BiTE, which was more effective than 8H9-BiTE in 14 different cancer cell lines. B11-BiTE also exhibited strong ADCC/ADCP. Therefore, the fully human B11-BiTE is a promising candidate for treatment of tumors expressing CD276.

Introduction

CD276 (B7-H3) is overexpressed on many different types of cancer cells and has been considered as a potential therapeutic target [1]. It is a type I transmembrane protein that belongs to the B7 superfamily of immunoregulatory proteins [2-4]. The human variant has two main isoforms, 4Ig-CD276 and 2Ig-CD276. 4Ig-CD276 has four Ig-like domains (V1, C1, V2 and C2) and is expressed more broadly and at higher levels compared to 2Ig-CD276 [5,6]. CD276 is involved in T cell activation and proliferation and is also detected in natural killer cells, B cells, and dendritic cells [3]. The role of CD276 in regulation of T cell-mediated adaptive immunity is complex and has not been completely elucidated [7]. In contrast, the involvement of CD276 in cancer progression is more consistent. It is overexpressed in many cancer types and the tumor stroma whereas low in normal tissue [8,9]. High expression of CD276 is associated with the presence of metastatic cancers [10], poor prognosis and high mortality [11]. CD276 promotes tumor proliferation, migration, invasion, development of cancer stem cell enrichment and drug resistance [12-14]. Blocking CD276 limits tumor growth and is synergistic with blocking of PD-1/PD-L1 [15,16]. The role of CD276 in tumor progression and the effect of its blockade on tumor growth has made it a desirable target for development of therapeutics.

Currently, there are several antibodies against CD276 in clinical trials such as enoblituzumab (MGA271) [17], orlotamab (MGD009) used as bispecific DART (anti-B7-H3)x(anti-CD3) [18], Ds-7300a used as antibody-drug conjugate (ADC) with the tropoisomerase I inhibitor Dxd [19] and ^{131}I-omburtamab [20]. ^{131}I-omburtamab, which utilizes the humanized murine monoclonal antibody 8H9, is in the most advanced stage of approval. There are also several clinical trials for CAR T cell adoptive therapies targeting CD276: 4SCAR-276 (NCT04432649) with sponsor Shenzhen Geno-Immune Medical Institute; 4–1BBζ B7H3-EGFRt-DHFR (NCT04483778) and SCRI-CARB7H3(s) (NCT04185038) with sponsor Seattle Children's Hospital. The pipeline of CD276 targeting antibody-based therapeutics also includes a variety of investigative formulations at different stages of development such as the ADCs (m276-MMAE) [9], (m276-SL-PBD) [21] and (MGC018-duocarmycin) [22], the bispecific B7-H3/CD16 [23], B7-H3/4–1BB [24], and several CAR T cell constructs [23,25-28]. Most of the above anti-CD276 antibodies are of murine origin with the potential for inducing an immune response, which in turn could reduce their efficacy [29]. Therefore, in this study we developed the CD276/CD3 bispecific T

* Corresponding author.
E-mail addresses: xianglei922@sina.com (X. Liu), mit666666@pitt.edu (D.S. Dimitrov).

https://doi.org/10.1016/j.tranon.2021.101232
Received 14 July 2021; Accepted 24 September 2021

cell engager B11-BiTE using the fully human antibody B11.

Our goal was to develop a BiTE, which is similar or more effective than the BiTE utilizing 8H9. We selected 8H9 for comparison because of its advanced progress in approval by the FDA. In order to achieve our goal, we constructed a large size (10^{11}) fully human phage-displayed single chain variable fragments (scFv) library. Clone B11 was selected after testing multiple clones for their ability to bind competitively with 8H9 and with similar strength to recombinant CD276. IgG-formats of B11-BiTE and 8H9-BiTE were constructed and tested on 14 cancer cell lines representing different cancer types including solid tumors. B11-BiTE showed similar or better performance compared to 8H9-BiTE, which demonstrated its suitability for further development.

Results

Broad expression of CD276 on different tumor cells and tissues

We first collected the normalized CD276 gene expression in primary tumors and paired normal tissues data from the TCGA, TARGET, and GTEX datasets. The results showed higher expression in primary tumors than in respective paired normal tissues (Figure S1A). This was significant ($p<0.005$) for CD276 overexpression in cancer *versus* normal in the bile duct, colon, esophagus, brain, head and neck, kidney, lung, pancreas, bone, skin, stomach, testis, and thymus. The expression of CD276 in different cancer cell lines was also examined, including the human prostate cancer cell lines DU145 and PC-3, bladder cancer cell lines T24 and HT1376, lung cancer cell line A549, hepatocellular carcinoma cell line Hep G2, breast cancer cell line MDA-MB-231, cervical cancer cell line Hela, malignant melanoma cell line A375, colorectal carcinoma HCT116, Ewing's sarcoma cell line EW-8, istiocytic lymphoma cell line U-937, biphenotypic B myelomonocytic leukemia cell line MV-4–11, chronic myelogenous leukemia (CML) cell line K562, Burkitt's lymphoma cell line Raji, Chinese hamster ovary cell CHO-K1 and human embryonic kidney HEK293T cells, they were stained by 8H9 and tested by flow cytometry. These results demonstrated that CD276 was widely over-expressed in most cancer cell lines, with low expression only in the K562 cell line (Fig. S1B). Further, CD276 is over-expressed in HEK293T cells, while there is no expression in Raji and CHO-K1 cells.

Characterization and epitope prediction of the CD276 binder B11

After panning using our in house fully human scFv phage display library, clone B11 was identified and it bound to human 2Ig-CD276 and cynomolgus 4Ig-CD276 with an EC_{50} of 30 nM and 25 nM (Fig. 1A), respectively. While it didn't bind to mouse 2Ig-CD276, and didn't show non-specific binding to human PD-L1, which also belongs to B7 family with CD276 (Fig. 1A). Overall, we characterized a fully human antibody B11 that can bind to human CD276 with high specificity. To predict the epitope of B11, we made 4 separate domain expressing stable cell lines: CHO-K1-C1, CHO-K1-C2, CHO-K1-V1, and CHO-K1-V2 (Fig. S2). B11 showed strong binding to CHO-K1-V1, weak binding to CHO-K1-V2, and no binding to the other two C1/C2-domain cell lines (Fig. 1B). The epitope of 8H9 has been reported to be the IRDF of the FG loop in the V1/V2 domain of CD276 [30]. To verify the epitope of B11 further, competitive ELISA with 8H9 was carried out. The results indicate that B11 competed with 8H9 for binding to full length CD276 (Fig. 1C). This competition was also confirmed by Blitz (Fig. 1D), where B11 failed to be associated after association of 8H9 to CD276. Additionally, competitive FACS for binding to CHO-K1-CD276 cell line (Fig. 1E, Fig. S3) confirmed again that B11 can block the binding sites of 8H9. These data corroborate that the B11 epitope is the V1/V2 domain of CD276, and it competes with 8H9 for binding to CD276.

Construction and characterization of B11-BiTE

An IgG format BiTE was constructed, in which humanized OKT3 was added at the C-terminus of the light chain of the B11-IgG (Fig. 2A). The proteins were analyzed by size exclusion chromatography (SEC) analysis, which confirmed the protein B11-BiTE was expressed successfully with bigger molecular weight (~200 kDa) than B11-IgG (~150 kDa). The purity was >95% with few multimers (Fig. 2B), which were also found by DLS (Fig. 2C), while the intensity of multimers reduced after 7 days of incubation at 37 °C. These data indicate that the B11-BiTE was easily produced and the protein showed good stability and aggregation-resistance. The avidity of B11-BiTE for binding to CD276 was compared

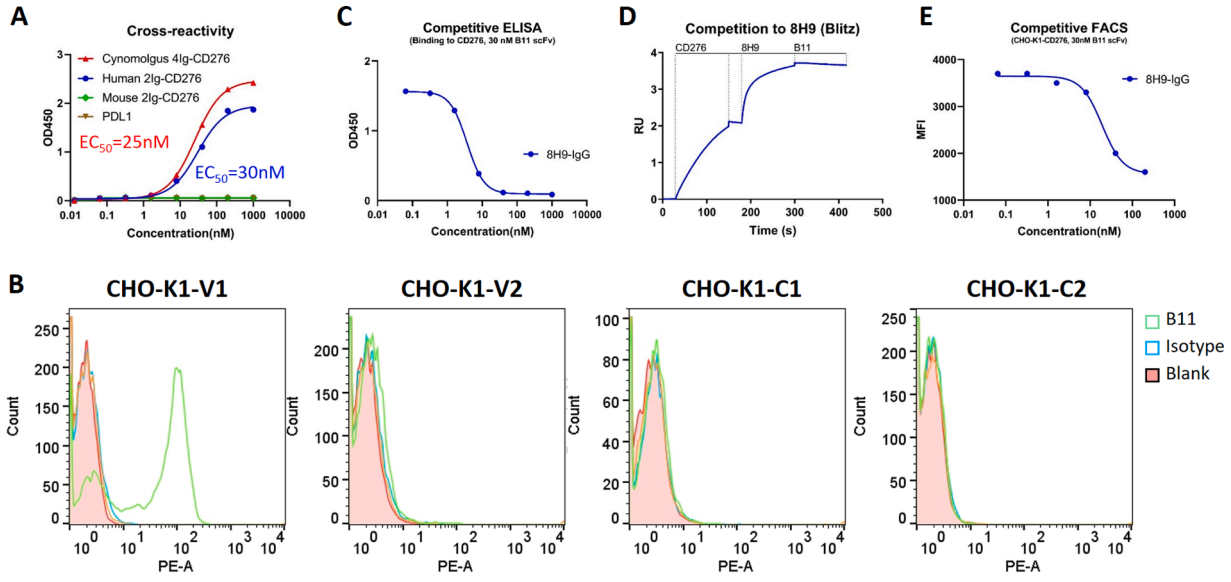

Fig. 1. Characterization and epitope mapping of B11. (A) Cross-reactivity of B11 scFv to human 2Ig-CD276, Cynomolgus 4Ig-CD276, mouse 2Ig-CD276 and human PD-L1 by ELISA. **(B)** The binding of B11 scFv to separate CD276 domain expressing cell lines. The bound B11 scFv was detected by anti-His-PE secondary antibody. **(C)** Competitive ELISA of B11 scFv with serially diluted 8H9-IgG for binding to 4Ig-CD276. After washing, the bound B11 scFv was detected by HRP conjugated anti-Flag antibody. **(D)** Competitive Blitz of B11 scFv with 8H9. After first association of 8H9 to 4Ig-CD276, B11 scFv was added for second association. **(E)** Competitive FACS of B11 scFv with serially diluted 8H9-IgG for binding to CHO-K1-CD276 cell line. The bound B11 scFv was detected by anti-Flag-PE secondary antibody. The mean fluorescent intensity (MFI) was analyzed by FlowJo 10 (related with Fig. S3) and the binding curve was made by GraphPad Prism 8.

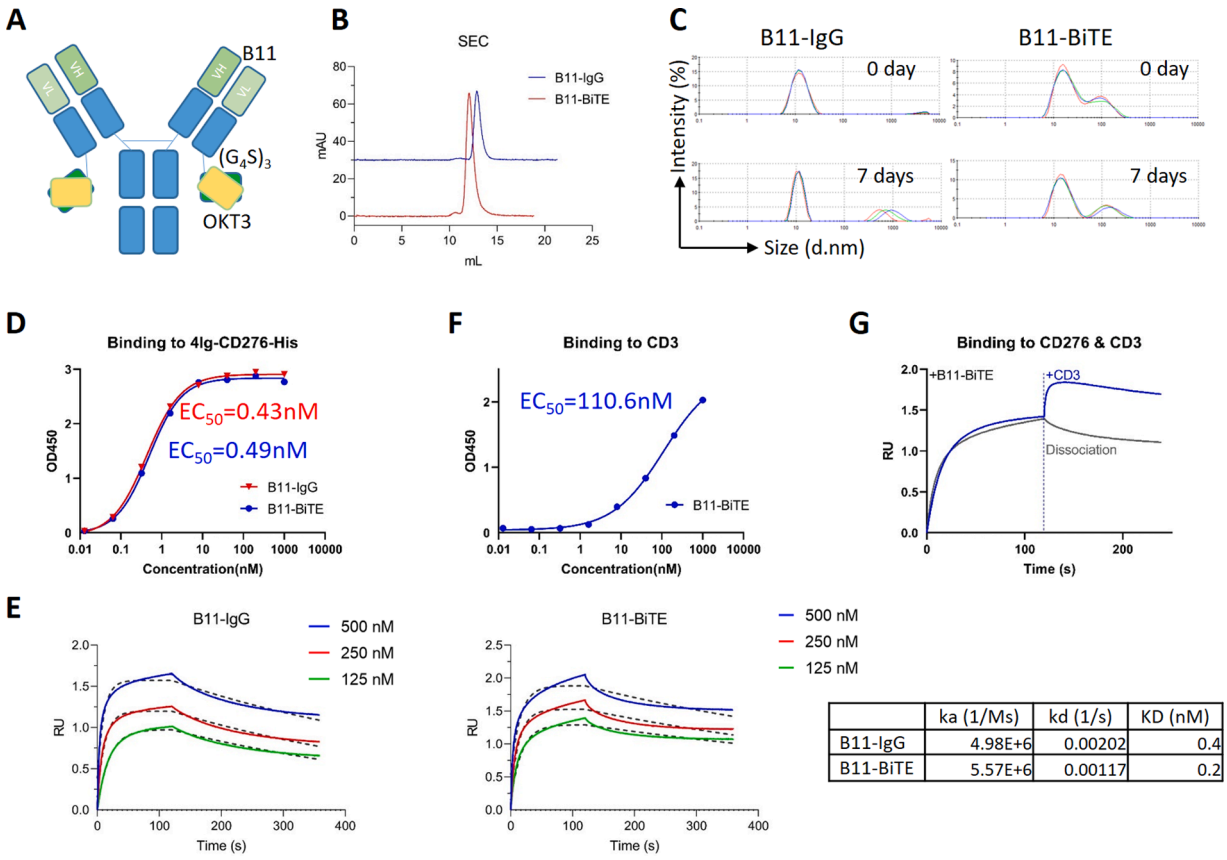

	ka (1/Ms)	kd (1/s)	KD (nM)
B11-IgG	4.98E+6	0.00202	0.4
B11-BiTE	5.57E+6	0.00117	0.2

Fig. 2. Characterization of B11-BiTE. (A) The structure illustration of B11-BiTE. Humanized OKT3 was ligate to C-terminal of B11-IgG light chain by $(G_4S)_3$. **(B)** Size exclusion chromatography (SEC) analysis of B11-IgG and B11-BiTE proteins. About 200 uL filtered proteins (1 mg/mL) in PBS were eluted by DPBS buffer at a flow rate of 0.4 mL/min. **(C)** Dynamic light scattering (DLS) analysis of B11-IgG and B11-BiTE. 500 μL proteins (1 mg/mL) were incubated at 37 °C for 7 days. **(D)** ELISA measurement of binding of B11-IgG and B11-BiTE to human 4Ig-CD276-His. **(E)** Sensorgrams for B11-IgG and B11-BiTE binding to 4Ig-CD276-Fc. Biotinylated 4Ig-CD276-Fc was coated on Biotin sensor and B11-IgG and B11-BiTE were used for binding. The k_a and k_d values were obtained by fitting to achieve the fitting parameter $R^2 > 0.99$. **(F)** ELISA measurement for B11-BiTE binding to human CD3. **(G)** Sensorgrams for B11-BiTE binding to 4Ig-CD276 and CD3. After first association of B11-BiTE to 4Ig-CD276, CD3 was added for second association, compared with regular sensorgram in Fig. 3E (125 nM).

with B11-IgG side by side. The EC_{50} of B11-IgG and B11-BiTE were 0.43 nM and 0.49 nM, respectively (Fig. 2D), and the K_D values were 0.4 nM and 0.2 nM, respectively (Fig. 2E). These data indicate that the addition of OKT3 didn't influence the avidity to B11-BiTE for binding to CD276. Moreover, B11-BiTE also can bind to CD3 protein with avidity of ~110.6 nM (Fig. 2F). Based on two-step association Blitz, B11-BiTE can bind to CD276 and CD3 simultaneously (Fig. 2G), which is essential to redirect T cells to tumor cells for T cell-mediated cytotoxicity. In summary, the function of B11-BiTE is good and can be used to redirect the T cells to tumor cells.

T cell-mediated cytotoxicity induced by the B11-BiTE

The T cell-mediated cytotoxicity induced by the B11-BiTE was evaluated next. Dose-dependent lysis was observed in cancer cells in the presence of B11-BiTE and 8H9-BiTE, while not in isotype control (Fig. 3). In 14 different cancer cell lines as verified above B11-BiTE had similar cytotoxicity with 8H9-BiTE, with IC_{50} ranging from 0.1~10 nM. B11-BiTE showed better cytotoxicity than 8H9-BiTE in the prostate cancer cell line DU145, lung cancer cell line A549, cervical cancer cell line Hela, Biphenotypic B myelomonocytic leukemia cell line MV-4–11, and human HEK293T cells. Moreover, B11-BiTE also induced T cell-mediated cytotoxicity to CD276 low-expression cell line K562, while 8H9-BiTE didn't. In the CHO-K1-CD276 stable cell line, the IC_{50} of B11-BiTE can reach to 0.77 pM, which is ~3-fold lower than 2.1 pM of 8H9-BiTE. Taken together, the high cytotoxic efficacy suggests the potential for antibody B11 therapeutics for CD276 overexpressing solid tumors.

Cytokine release by T cells and ADCC/ADCP

To further analyze the *in vitro* mechanism of T cell-mediated cytotoxicity induced by B11-BiTE, key cytokine secretion was assessed after 24 h co-incubation of CHO-K1-CD276 cells and T cells at an E:T ratio of 10:1. Dose-dependent release of cytokines was observed by T cells in the presence of B11-BiTE and 8H9-BiTE (Fig. 4A). Moreover, significantly higher amounts TNF-α and slightly higher amounts of IFN-γ were produced in the culture supernatants in the presence of B11-BiTE than 8H9-BiTE. These data indicate that CD276 redirection promotes T cells to kill tumor cells by cytokine release. As an IgG-format BiTE, effector function induced by Fc region also can be an important strategy for cancer therapy, so ADCC/ADCP functions of B11-BiTE were studied using a bioluminescent reporter assay, and the results showed that B11-BiTE can induce strong ADCC/ADCP activation with EC50 1~10 pM (Fig. 4B).

Discussion

CD276 is an attractive target for cancer immunotherapy [31] because it is expressed as a pan-target at high levels in tumor cells (Fig. S1). Consequently, a panel of CD276-specific antibodies have shown potent antitumor activity. However, most of the anti-CD276 antibodies are of murine origin or have been humanized, which have higher potential for immunogenicity in humans. In our study, we aimed to develop fully human antibodies that targeting CD276 using our large size, fully human phage-displayed scFv library. We identified clone B11 that has specific high avidity binding to human CD276 in an IgG1 format

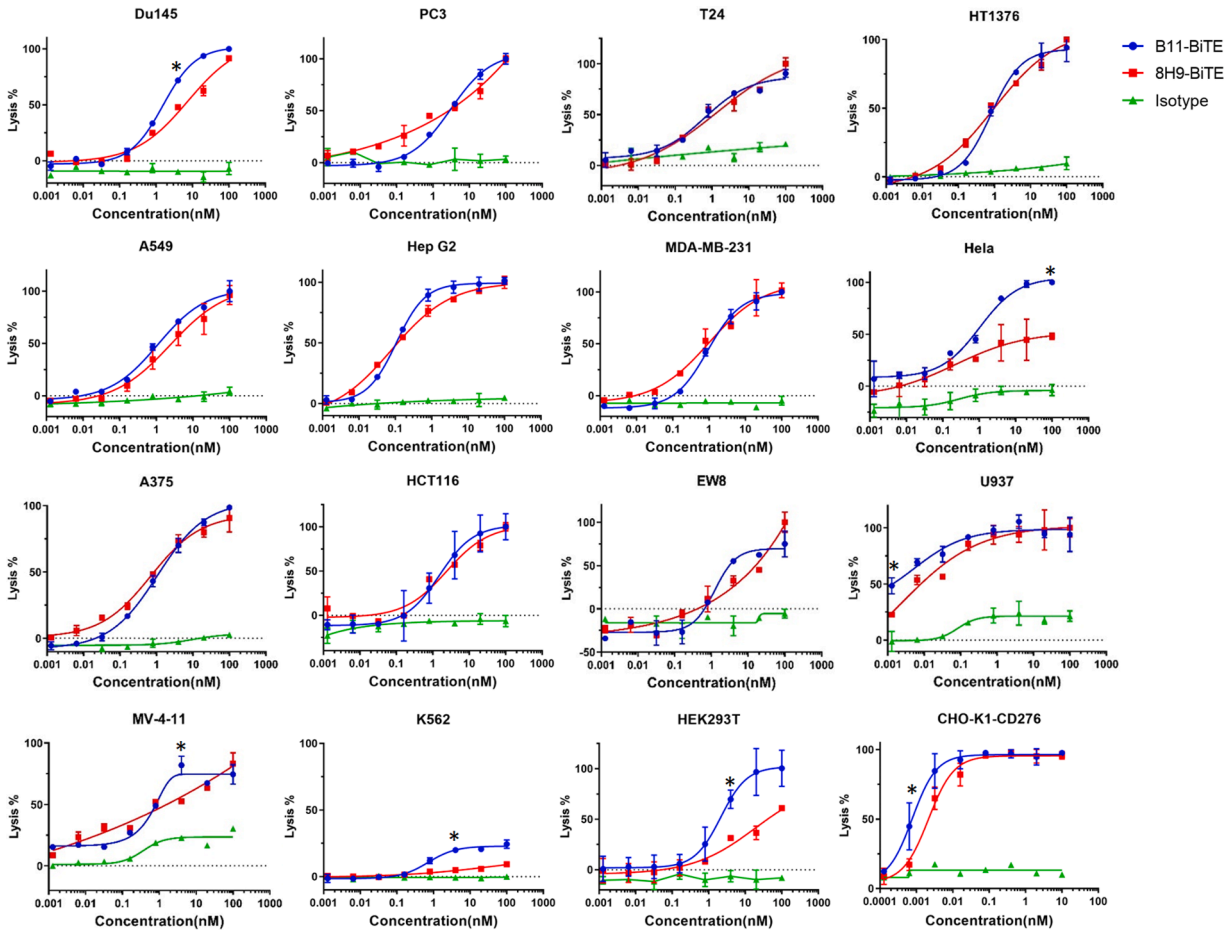

Fig. 3. Cytotoxic of T cells to cancer cell lines induced by B11-BiTE and 8H9-BiTE. Target cells (10,000 cells/well) were mixed with serially diluted BiTE antibodies in 96-well plates. Activated T cells were added to the wells at E:T ratio 10:1 and cultured for 24 h. The luminescence signal was measured and used for calculate percent cytotoxicity (lysis%). Curves were fitted using a four-parameter logistic fitting with GraphPad Prism 8.

(K_D 0.4 nM, Fig. 2). We confirmed that B11 bound to V1/V2 domain of CD276 and showed strong competition with 8H9. The epitope of 8H9 has been reported to bind to the IRDF sequence of the FG loop in the V1/V2 domain of CD276 [30]. The FG loop of CD276 is important for CD276-mediated inhibition of T cell proliferation [32].

BiTE is a promising strategy for immune checkpoint therapy that designed to directly activate T cells against malignancies [33]. Zheng M et al. found that anti-CD276/CD3 BiTE effectively targeted and killed nasal natural killer/T cell lymphoma (NKTCL) cells *in vitro*, and suppressed the growth of NKTCL tumors in NSG mouse models. [34]. Li H et al. also verified that CD276 × CD3 BiTE specifically and efficiently redirected their cytotoxicity against CD276 overexpressing tumor cells both *in vitro* and in xenograft mouse models [35]. Besides BiTE, Liu J et al. tried bispecifc killer cell engager (BiKE) and found that BiKE improved antitumor efficacy mediated by NK cells *in vitro* and *in vivo* [23]. To verify the efficacy of B11, we constructed B11-BiTE, also 8H9-BiTE as control. The B11-BiTE protein is easily produced and showed good stability and aggregation-resistance (Fig. 2). A T cell cytotoxicity assay was carried out to verify the efficacy of B11-BiTE *in vitro*. As a pan-tumor antigen, we assayed 14 different tumor cell lines. It is promising that B11-BiTE induced T cell killing to every tumor cell line in a dose-dependent manner. B11-BiTE's cytotoxicity was similar to or even better than 8H9-BiTE, especially in prostate cancer cell line DU145, lung cancer cell line A549, cervical cancer cell line Hela, biphenotypic B myelomonocytic leukemia cell line MV-4–11, and human HEK293T cells (Fig. 3). The IC_{50} ranged from 0.1 to10 nM, which may cause by different expression levels of CD276. In the high-expression stable cell line CHO-K1-CD276, the IC_{50} of B11-BiTE is ~3-fold lower than 8H9-BiTE (0.77 pM *vs* 2.1 pM, $p<0.05$), thus indicating the excellent efficacy of B11-BiTE *in vitro*. The key cytokine TNF-α and IFN-γ production confirmed again the advantage of B11-BiTE over 8H9-BiTE (Fig. 4A), which promoted T cells to kill tumor cells by releasing more cytokines. As an IgG-format BiTE, ADCC/ADCP functions induced by Fc region were also important for cytotoxicity to tumor cells, and B11-BiTE retained these functions (Fig. 4B).

Taken together, here we report a fully human antibody B11 that has high affinity to CD276 with an epitope in the V1/V2 domain of CD276. B11-BiTE can induce T cell-mediated cytotoxicity to different cancer cell lines *in vitro*. The high efficacy and fully human origin suggest therapeutic potential of B11 for CD276 overexpressing solid tumors.

Materials and methods

Cell lines and cell culture

The human prostate cancer cell lines DU145 (HTB-81™) and PC-3 (CRL-1435™), bladder cancer cell lines T24 (HTB-4™) and HT1376 (CRL-1472™), the lung cancer cell line A549 (CCL-185™), hepatocellular carcinoma cell line Hep G2 (HB-8065™), breast cancer cell line MDA-MB-231 (CRM-HTB-26™), cervical cancer cell line Hela (CCL-2™), malignant melanoma cell line A375 (CRL-1619™), colorectal carcinoma HCT116 (CCL-247™), istiocytic lymphoma cell line U-937 (CRL-1593.2™), biphenotypic B myelomonocytic leukemia cell line MV-4–11 (CRL-9591), chronic myelogenous leukemia (CML) cell line K562 (CCL-243™), Burkitt's lymphoma cell line Raji (CCL-86™), Chinese hamster ovary cell CHO-K1 (CCL-61™) and human embryonic kidney

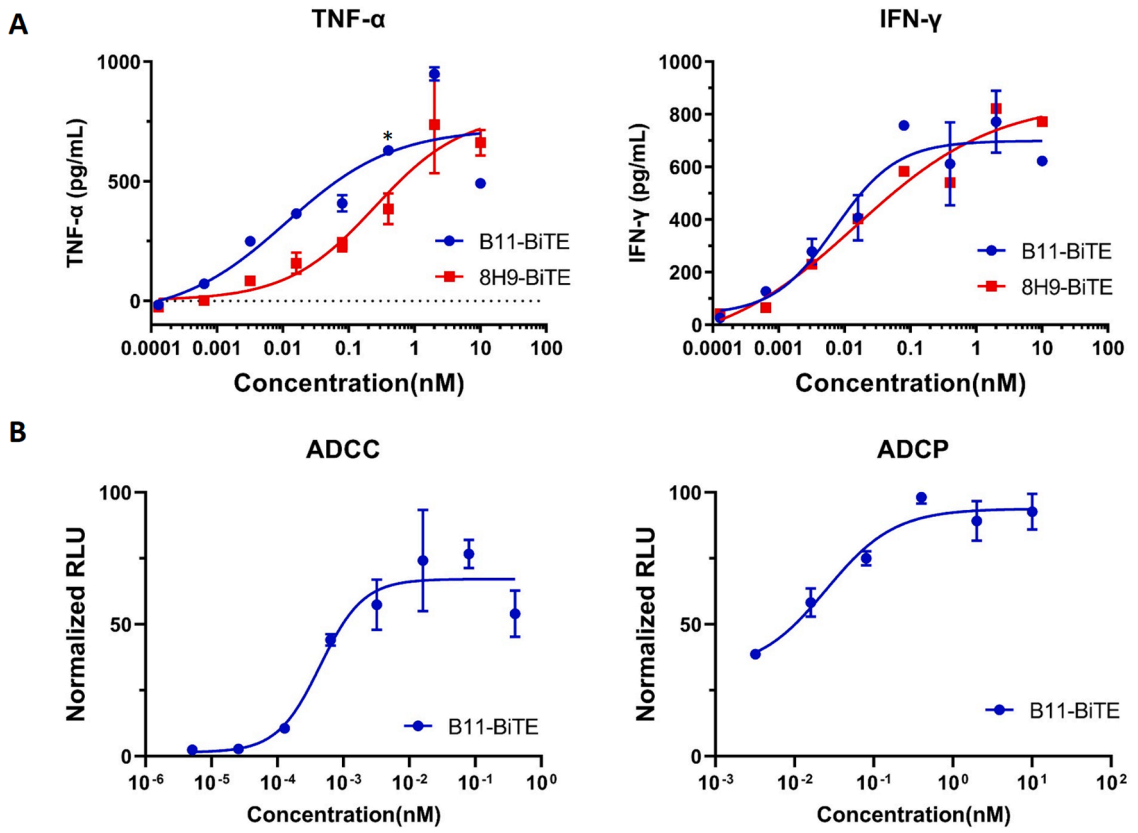

Fig. 4. Cytokine release and ADCC/ADCP assays induced by B11-BiTE. (A) Target cells CHO-K1-CD276 (10,000 cells/well) were mixed with serially diluted BiTE antibodies in 96-well plates. Activated T cells were added to the wells at E:T ratio 10:1 and cultured for 24 h. The supernatants were harvested for cytokine production assayed by ELISA. **(B)** ADCC/ADCP function was measured using a bioluminescent reporter assay, results are expressed in normalized relative luciferase units (RLU). Curves were fitted using a four-parameter logistic fitting with GraphPad Prism 8.

HEK293T (CRL-11,268™) were purchased from the ATCC (Manassas, VA, USA). The Ewing's sarcoma cell line EW-8 was previously acquired by our lab. All the cell lines were cultured at 37 °C in a 5% CO_2 humidified atmosphere in proper medium following supplier instructions supplemented with 10% fetal bovine serum (FBS, Gibco) and 1% Penicillin/Streptomycin (P/S, Gibco).

Genes of full length human 4Ig-CD276 (Genescript, Piscataway, NJ) or separate domain genes C1, C2, V1 or V2 were amplified and fused with Flag-tag gene at N-terminal [36], then subcloned into pSecTag B (Invitrogen) and used to construct stable cell line CHO-K1-CD276, domain expressing cell lines CHO-K1-C1, CHO-K1-C2, CHO-K1-V1, and CHO-K1-V2. The stable cell lines were cultured in F-12 K medium (Gibco) with 10% FBS, 1% P/S and 200 μg/ml zeocin (Thermo Fisher, Waltham, MA). CHO-K1-CD276-Luci is constructed that expressing luciferase based on CHO-K1-CD276.

CD276 gene expression analysis

Normalized CD276 gene expression data from the TCGA, TARGET, and GTEX datasets were downloaded as $\log_2$(normalized counts +1) from the UCSC Xena Browser [37]. Gene expression data analysis and graphing were performed in GraphPad Prism 9. Only tissues with paired normal and primary tumor data were used to make the heat map and calculate significant differences (Mann-Whitney, significance was defined as $P < 0.05$).

Production of BiTE proteins

The anti-CD276 monoclonal antibody (mAb) sequence used in BiTE vectors was derived from a highly specific single-chain variable fragment (scFv) against B7-H3 (clone B11) generated by panning from our phage display library. To make B11-BiTE, humanized OKT3 (synthesized by IDT, Coralville, Iowa) was inserted at the C-terminal of light chain of B11-IgG with $(G_4S)_3$ linker [38]. The B11-IgG or BiTE proteins were expressed in the Expi293™ expression system (Thermo Fisher Scientific) and purified by protein A resin (GenScript, Piscataway, NJ). Protein purity was estimated as >95% and protein concentration was measured spectrophotometrically (NanoVue, GE Healthcare). Positive control 8H9-BiTE and isotype control (binding to other unrelated antigen) proteins were expressed and purified using the same methods.

ELISA

Antigen proteins human 4Ig-CD276-His, 2Ig-CD276-Fc, PD-L1-His, Cynomolgus 4Ig-CD276-His, mouse 2Ig-CD276-His (Sino biological, Wayne, PA), CD3ε&δ-His (Acro, Newark, DE) were coated separately on 96-well plates (Costar) at 200 ng/well in PBS overnight at 4 °C. The plate was blocked using 3% skim milk for 1 h at room temperature (RT). Serially diluted B11 antibodies (scFv, IgG or BiTE) were then added and incubated for 2 h at RT. The plates are washed 4 times with 0.05% tween in phosphate buffered saline (PBST). Anti-Flag (for scFv) or anti-human Fc (for IgG or BiTE) horseradish peroxidase (HRP) conjugated secondary antibody (Sigma-Aldrich) was added to the plate followed by incubation for 1 h at RT. After another 4 washes with PBST, the plate was incubated with 3,3′,5,5′-tetramethylbenzidine substrate solution (TMB, Sigma-Aldrich) for 3 min. The reaction was stopped using 1 M H_2SO_4 followed by reading absorbance of each well at 450 nm. For the competitive ELISA, 30 nM B11 scFv (Flag-tag) was incubated with serially diluted 8H9-IgG, and the mixtures were added to CD276-His coated wells. After washing, bound B11 scFv was detected by anti-Flag-HRP

secondary antibody (Sigma-Aldrich). Curves were fitted using a four-parameter logistic fitting with GraphPad Prism 8.

Blitz

Antibody affinities and avidities were analyzed by the biolayer interferometry BLItz (ForteBio, Menlo Park, CA). 4Ig-CD276-Fc was biotinylated with EZ-link sulfo-NHS-LC-biotin (Thermo Fisher, Waltham, MA) to get CD276-Fc-Bio. Streptavidin biosensors (ForteBio: 18–5019) were coated with CD276-Fc-Bio for 2 min and incubated in DPBS (pH = 7.4) to establish baselines. For avidity measurements, 125 nM, 250 nM and 500 nM B11-IgG/BiTE were chosen for association. The association was monitored for 2 min and then the antibody allowed to dissociate in DPBS for 4 min. The ka and kd were derived from the sensorgrams fitting and used for K_D calculation. For the competitive binding Blitz, 8H9 were associated first and then B11 were used for 2nd association for 2 min. To test the binding of B11-BiTE to CD276 and CD3 simultaneously, after the association of 125 nM B11-BiTE was incubated in DPBS (pH = 7.4) for 30 s to establish baselines again, then 50 ug/ml CD3ε&δ (Acro, Newark, DE) was used for the 2nd association (2 min).

Flow cytometry

To detect CD276 expression in different cell lines, 8H9 scFv (Flag tag, 500 nM) were incubated with cells for 30 min at 4 °C. Cells were washed and then incubated with PE conjugated anti-Flag antibody (Sigma-Aldrich) for 30 min at 4 °C. Bound 8H9 were detected by flow cytometry using BD LSR II (San Jose, CA). For CHO-K1-CD276, CHO-K1-C1, CHO-K1-C2, CHO-K1-V1, and CHO-K1-V2 stable cell lines, PE conjugated anti-Flag antibody was used to confirm the expression of CD276 or domains. For competitive binding to CHO-K1-CD276 cell, 30 nM B11 scFv (Flag-tag) was incubated with serially diluted 8H9-IgG, and the mixtures were incubated with cells. After washing, bound B11 scFv was detected by anti-Flag-PE secondary antibody (Sigma-Aldrich). The mean fluorescent intensity (MFI) was analyzed by FlowJo 10 and the binding curve was made by GraphPad Prism 8.

Size exclusion chromatography (SEC)

The ÄKTA pure chromatography system (GE Healthcare) was used. The column (Superdex 200 Increase 10/300 GL) was calibrated with protein molecular mass standards of Thyroglobulin (Mr 669,000 kDa), Ferritin (Mr 440,000 kDa), Aldolase (Mr 158,000 kDa), Conalbumin (Mr 75,000 kDa), Ovalbumin (Mr 44,000 kDa), Carbonic anhydrase (Mr 29,000 kDa), Ribonuclease A (Mr 13,700 kDa). About 200 uL of filtered proteins (1 mg/mL) in PBS were used for analysis. Protein was eluted by DPBS buffer at a flow rate of 0.4 mL/min.

Dynamic light scattering (DLS)

For evaluation of aggregation propensity, B11-IgG and BiTE in DPBS were filtered through a 0.22 μm filter. The concentration was adjusted to 1 mg/mL; 500 μL samples were incubated at 37 °C. On day 0 and day 7, samples were taken out for DLS measurement on the Zetasizer Nano ZS ZEN3600 (Malvern Instruments Limited, Westborough, MA) to determine the size distributions of protein particles.

T cell isolation and activation

Human primary T cells were isolated from normal human donor peripheral blood mononuclear cells (PBMCs, Zen-Bio, Durham, NC) using CD3 MicroBeads (Miltenyi Biotec, Auburn, CA), and were further activated by T Cell TransAct (Miltenyi Biotec, Auburn, CA) for 48 h following the manufacturer's instructions. The T cells were cultured in TexMACS™ Medium (Miltenyi Biotec, Auburn, CA) with 50 U/mL recombinant human interleukin (IL)−2 (Miltenyi Biotec, Auburn, CA) at 37 °C in a humidified atmosphere with 5% CO_2. Cells were used for cytotoxicity assays between day 4 and day 8 of culture.

Cytotoxicity assays

Cytotoxicity of T cells induced by BiTE was measured using the dead-cell protease release method. Briefly, target cells (10,000 cells/well) were mixed with serially diluted BiTE antibodies in 96-well white plates (Corning) in 50 μL of growth medium. Activated T cells (50 μL) were added to the wells at effector to target (E:T) ratio 10:1 and cultured for 24 h at 37 °C in a 5% CO_2 humidified atmosphere. CytoTox-Glo™ Cytotoxicity Assay kit (Promega, Madison, WI) was used to measure the relative number of dead cells in cell populations following the manufacturer's instructions. A maximum lysis control was used where digitonin was added to target cell only wells before adding the lysis reagent. The luminescence signal was measured using BioTek synergy multimode reader (Winooski, VT). The percent cytotoxicity was calculated using the following formula:% Lysis = 100 × (Experimental signal – Untreated cells signal)/(Maximum signal – Untreated cells signal). For CHO-K1-CD276-Luci cells, the luciferase signal was measured using Bright-Glo Luciferase Assay System (Promega, Madison, WI) following the manufacturer's instructions. The percent cytotoxicity was calculated using the following formula:% Lysis = 100 × (1-Experimental signal / Untreated cells signal). Curves were fitted using a four-parameter logistic fitting with GraphPad Prism 8.

Cytokine release assay

Cells were prepared the same as the cytotoxicity assays. After 24 h of culturing cells, the supernatant was harvested for cytokine production and assayed using IFN gamma Human ELISA Kit and TNF alpha Human ELISA Kit (Thermo Fisher) following the manufacturer's instructions. Curves were fitted using a four-parameter logistic fitting with GraphPad Prism 8.

ADCC/ADCP reporter bioassay

Antibody-dependent cellular cytotoxicity (ADCC) and antibody-dependent cellular phagocytosis (ADCP) function was measured using a bioluminescent reporter assay (ADCC Reporter Bioassay and FcγRIIa-H ADCP Bioassay, Promega) following the manufacturer's instructions. Briefly, target cell CHO-K1-CD276 (10,000 cells/well) were mixed with serially diluted B11-BiTE in 96-well white plates (Corning) in 50 μL of growth medium. Engineered Jurkat-FcγRIIIa-V158 cells or Jurkat-FcγRIIa-H cells (50 μL) were added to the wells at E:T ratio 5:1 and cultured for 4 h at 37 °C in a 5% CO_2 humidified atmosphere. Finally, luciferase production was measured using a luminescent substrate (Bright Glo, Promega). Results are expressed in relative luciferase units (RLU), normalized RLU is calculated by assigning 100% to the maximum bioluminescent signal. Curves were fitted using a four-parameter logistic fitting with GraphPad Prism 8.

Statistical analysis

All experiments were conducted in duplicate, significant differences were determined by one-way analysis of variance followed by Tukey's test, using the GraphPad Prism 8 package. Statistical significance was defined as *($P < 0.05$).

Declaration of Competing Interest

The authors declare no conflict of interest.

Acknowledgments

We thank the members of the Center for Antibody Therapeutics: Wei

Li, Zehua Sun, Xiaojie Chu, Du-San Baek, and Yae-Jin Kim for helpful discussions. This work was supported by the UPMC.

Author contributions

DSD, XL, DZ and JWM conceived and designed the research; XL performed most research; DZ panned the library to identify the antibody, CA performed gene expression analysis, CC helped with the protein expression. XL, DZ and CA wrote the first draft of the article, and all authors discussed the results and contributed to the manuscript.

Supplementary materials

Supplementary material associated with this article can be found, in the online version, at doi:10.1016/j.tranon.2021.101232.

References

[1] A. Pant, R. Medikonda, M. Lim, Alternative checkpoints as targets for immunotherapy, Curr. Oncol. Rep. 22 (2020) 126, https://doi.org/10.1007/s11912-020-00983-y.

[2] K. Flem-Karlsen, Ø. Fodstad, C.E. Nunes-Xavier, B7-H3 immune checkpoint protein in human cancer, Curr. Med. Chem. 27 (2020) 4062–4086, https://doi.org/10.2174/0929867326666190517115515.

[3] P. Steinberger, O. Majdic, S.V. Derdak, K. Pfistershammer, S. Kirchberger, C. Klauser, G. Zlabinger, W.F. Pickl, J. Stockl, W. Knapp, Molecular characterization of human 4Ig-B7-H3, a member of the B7 family with four Ig-like domains, J. Immunol. 172 (2004) 2352–2359.

[4] S. Yang, W. Wei, Q. Zhao, B7-H3, a checkpoint molecule, as a target for cancer immunotherapy, Int. J. Biol. Sci. 16 (2020) 1767–1773, https://doi.org/10.7150/ijbs.41105.

[5] F. Kontos, T. Michelakos, T. Kurokawa, A. Sadagopan, J.H. Schwab, C.R. Ferrone, S. Ferrone, B7-H3: an attractive target for antibody-based immunotherapy, Clin. Cancer Res. (2020), https://doi.org/10.1158/1078-0432.Ccr-20-2584, 10.1158/1078-0432.Ccr-20-2584, clincanres.2584.2020.

[6] Z. Wang, J. Yang, Y. Zhu, Y. Zhu, B. Zhang, Y. Zhou, Differential expression of 2IgB7-H3 and 4IgB7-H3 in cancer cell lines and glioma tissues, Oncol. Lett. 10 (2015) 2204–2208, https://doi.org/10.3892/ol.2015.3611.

[7] K.A. Hofmeyer, A. Ray, X. Zang, The contrasting role of B7-H3, Proc. Natl. Acad. Sci. U.S.A. 105 (2008) 10277–10278, https://doi.org/10.1073/pnas.0805458105.

[8] K. Flem-Karlsen, O. Fodstad, M. Tan, C.E. Nunes-Xavier, B7-H3 in cancer - beyond immune regulation, Trends Cancer 4 (2018) 401–404, https://doi.org/10.1016/j.trecan.2018.03.010.

[9] S. Seaman, Z. Zhu, S. Saha, X.M. Zhang, M.Y. Yang, M.B. Hilton, K. Morris, C. Szot, H. Morris, D.A. Swing, et al., Eradication of tumors through simultaneous ablation of CD276/B7-H3-positive tumor cells and tumor vasculature, Cancer Cell 31 (2017), https://doi.org/10.1016/j.ccell.2017.03.005, 501-515 e508.

[10] G. Amori, E. Sugawara, Y. Shigematsu, M. Akiya, J. Kunieda, T. Yuasa, S. Yamamoto, J. Yonese, K. Takeuchi, K. Inamura, Tumor B7-H3 expression in diagnostic biopsy specimens and survival in patients with metastatic prostate cancer, Prostate Cancer Prostatic Dis. (2021), https://doi.org/10.1038/s41391-021-00331-6.

[11] Z. Ye, Z. Zheng, X. Li, Y. Zhu, Z. Zhong, L. Peng, Y. Wu, B7-H3 overexpression predicts poor survival of cancer patients: a meta-analysis, Cell. Physiol. Biochem. 39 (2016) 1568–1580, https://doi.org/10.1159/000447859.

[12] Z. Liu, W. Zhang, J.B. Phillips, R. Arora, S. McClellan, J. Li, J.H. Kim, R.W. Sobol, M. Tan, Immunoregulatory protein B7-H3 regulates cancer stem cell enrichment and drug resistance through MVP-mediated MEK activation, Oncogene 38 (2019) 88–102, https://doi.org/10.1038/s41388-018-0407-9.

[13] P. Dong, Y. Xiong, J. Yue, S.J.B. Hanley, H. Watari, B7H3 as a promoter of metastasis and promising therapeutic target, Front. Oncol. 8 (2018) 264, https://doi.org/10.3389/fonc.2018.00264.

[14] T. Shi, Y. Ma, L. Cao, S. Zhan, Y. Xu, F. Fu, C. Liu, G. Zhang, Z. Wang, R. Wang, et al., B7-H3 promotes aerobic glycolysis and chemoresistance in colorectal cancer cells by regulating HK2, Cell Death Dis. 10 (2019) 308, https://doi.org/10.1038/s41419-019-1549-6.

[15] K. Yonesaka, K. Haratani, S. Takamura, H. Sakai, R. Kato, N. Takegawa, T. Takahama, K. Tanaka, H. Hayashi, M. Takeda, et al., B7-H3 negatively modulates CTL-mediated cancer immunity, Clin. Cancer Res. 24 (2018) 2653–2664, https://doi.org/10.1158/1078-0432.CCR-17-2852.

[16] Y.-h. Lee, N. Martin-Orozco, P. Zheng, J. Li, P. Zhang, H. Tan, H.J. Park, M. Jeong, S.H. Chang, B.-.S. Kim, et al., Inhibition of the B7-H3 immune checkpoint limits tumor growth by enhancing cytotoxic lymphocyte function, Cell Res. 27 (2017) 1034, https://doi.org/10.1038/cr.2017.90.

[17] E. Shenderov, A. Demarzo, K. Boudadi, M. Allaf, H. Wang, C. Chapman, C. Pavlovich, T. Bivalacqua, T.S. O'Neal, R. Harb, et al., Phase II neoadjuvant and immunologic study of B7-H3 targeting with enoblituzumab in localized intermediate- and high-risk prostate cancer, J. Clin. Oncol. 36 (2018), https://doi.org/10.1200/JCO.2018.36.15_suppl.TPS5099. TPS5099-TPS5099.

[18] S. Shankar, A.I. Spira, J. Strauss, L. Liu, R. La Motte-Mohs, T. Wu, S. Johnson, E. Bonvini, P.A. Moore, J.M. Wigginton, et al., A phase 1, open label, dose escalation study of MGD009, a humanized B7-H3 x CD3 DART protein, in combination with MGA012, an anti-PD-1 antibody, in patients with relapsed or refractory B7-H3-expressing tumors, J. Clin. Oncol. 36 (2018), https://doi.org/10.1200/JCO.2018.36.15_suppl.TPS2601. TPS2601-TPS2601.

[19] M. Yamato, J. Hasegawa, C. Hattori, T. Maejima, T. Shibutani, T. Deguchi, N. Izumi, A. Watanabe, Y. Nishiya, T. Nakada, et al., DS-7300a, a novel B7-H3-targeting antibody-drug conjugate with a novel DNA topoisomerase I inhibitor DXd, exhibits potent anti-tumor effects in nonclinical models, Eur. J. Cancer 138 (2020) S14–S15, https://doi.org/10.1016/S0959-8049(20)31102-3.

[20] S. Modak, P. Zanzonico, M. Grkovski, E.K. Slotkin, J.A. Carrasquillo, S. K. Lyashchenko, J.S. Lewis, I.Y. Cheung, T. Heaton, M.P. LaQuaglia, et al., B7H3-directed intraperitoneal radioimmunotherapy with radioiodinated omburtamab for desmoplastic small round cell tumor and other peritoneal tumors: results of a phase I study, J. Clin. Oncol. 38 (2020) 4283–4291, https://doi.org/10.1200/JCO.20.01974.

[21] N.M. Kendsersky, J.M. Lindsay, E.A. Kolb, M.A. Smith, B.A. Teicher, S. Erickson, E. J. Earley, Y.P. Mossé, D. Martinez, J. Pogoriler, et al., The B7-H3-targeting antibody-drug conjugate m276-SL-PBD is potently effective against pediatric cancer preclinical solid tumor models, Clin. Cancer Res. (2021), https://doi.org/10.1158/1078-0432.Ccr-20-4221 clincanres.4221.2020, doi:10.1158/1078-0432.Ccr-20-4221.

[22] J.A. Scribner, J.G. Brown, T. Son, M. Chiechi, P. Li, S. Sharma, H. Li, A. De Costa, Y. Li, Y. Chen, et al., Preclinical development of MGC018, a duocarmycin-based antibody-drug conjugate targeting B7-H3 for solid cancer, Mol. Cancer Ther. (2020), https://doi.org/10.1158/1535-7163.MCT-20-0116.

[23] J. Liu, S. Yang, B. Cao, G. Zhou, F. Zhang, Y. Wang, R. Wang, L. Zhu, Y. Meng, C. Hu, et al., Targeting B7-H3 via chimeric antigen receptor T cells and bispecific killer cell engagers augments antitumor response of cytotoxic lymphocytes, J. Hematol. Oncol. 14 (2021) 21, https://doi.org/10.1186/s13045-020-01024-8.

[24] G. You, Y. Lee, Y.-.W. Kang, H.W. Park, K. Park, H. Kim, Y.-.M. Kim, S. Kim, J.-.H. Kim, D. Moon, et al., B7-H3×4-1BB bispecific antibody augments antitumor immunity by enhancing terminally differentiated $CD8^{+}$tumor-infiltrating lymphocytes, Sci. Adv. 7 (2021) eaax3160, https://doi.org/10.1126/sciadv.aax3160.

[25] B. Moghimi, S. Muthugounder, S. Jambon, R. Tibbetts, L. Hung, H. Bassiri, M. D. Hogarty, D.M. Barrett, H. Shimada, S. Asgharzadeh, Preclinical assessment of the efficacy and specificity of GD2-B7H3 SynNotch CAR-T in metastatic neuroblastoma, Nat. Commun. 12 (2021) 511, https://doi.org/10.1038/s41467-020-20785-x.

[26] J. Theruvath, E. Sotillo, C.W. Mount, C.M. Graef, A. Delaidelli, S. Heitzeneder, L. Labanieh, S. Dhingra, A. Leruste, R.G. Majzner, et al., Locoregionally administered B7-H3-targeted CAR T cells for treatment of atypical teratoid/rhabdoid tumors, Nat. Med. (2020), https://doi.org/10.1038/s41591-020-0821-8.

[27] X. Tang, Y. Wang, J. Huang, Z. Zhang, F. Liu, J. Xu, G. Guo, W. Wang, A. Tong, L. Zhou, Administration of B7-H3 targeted chimeric antigen receptor-T cells induce regression of glioblastoma, Sig, Transd. Target. Ther. 6 (2021) 125, https://doi.org/10.1038/s41392-021-00505-7.

[28] R.G. Majzner, J.L. Theruvath, A. Nellan, S. Heitzeneder, Y. Cui, C.W. Mount, S. P. Rietberg, M.H. Linde, P. Xu, C. Rota, et al., CAR T cells targeting B7-H3, a pan-cancer antigen, demonstrate potent preclinical activity against pediatric solid tumors and brain tumors, Clin. Cancer Res. (2019), https://doi.org/10.1158/1078-0432.CCR-18-0432, 10.1158/1078-0432.CCR-18-0432 %J Clinical Cancer Research, clincanres.0432.2018%J Clinical Cancer Research.

[29] W.S. Putnam, S. Prabhu, Y. Zheng, M. Subramanyam, Y.M. Wang, Pharmacokinetic, pharmacodynamic and immunogenicity comparability assessment strategies for monoclonal antibodies, Trends Biotechnol. 28 (2010) 509–516, https://doi.org/10.1016/j.tibtech.2010.07.001.

[30] M. Ahmed, M. Cheng, Q. Zhao, Y. Goldgur, S.M. Cheal, H.F. Guo, S.M. Larson, N. K. Cheung, Humanized affinity-matured monoclonal antibody 8H9 has potent antitumor activity and binds to FG loop of tumor antigen B7-H3, J. Biol. Chem. 290 (2015) 30018–30029, https://doi.org/10.1074/jbc.M115.679852.

[31] Hahn, A.W.; Gill, D.M.; Pal, S.K.; Agarwal, N. The future of immune checkpoint cancer therapy after PD-1 and CTLA-4. 2017, 9, 681–692, doi:10.2217/imt-2017-0024.

[32] V. Vigdorovich, U.A. Ramagopal, E. Lazar-Molnar, E. Sylvestre, J.S. Lee, K. A. Hofmeyer, X. Zang, S.G. Nathenson, S.C. Almo, Structure and T cell inhibition properties of B7 family member, B7-H3, Structure 21 (2013) 707–717, https://doi.org/10.1016/j.str.2013.03.003.

[33] Z. Wu, N.V. Cheung, T cell engaging bispecific antibody (T-BsAb): from technology to therapeutics, Pharmacol. Ther. 182 (2018) 161–175, https://doi.org/10.1016/j.pharmthera.2017.08.005.

[34] M. Zheng, L. Yu, J. Hu, Z. Zhang, H. Wang, D. Lu, X. Tang, J. Huang, K. Zhong, Z. Wang, et al., Efficacy of B7-H3-redirected BiTE and CAR-T immunotherapies against extranodal nasal natural killer/T cell lymphoma, Transl. Oncol. 13 (2020), 100770, https://doi.org/10.1016/j.tranon.2020.100770.

[35] H. Li, C. Huang, Z. Zhang, Y. Feng, Z. Wang, X. Tang, K. Zhong, Y. Hu, G. Guo, L. Zhou, et al., MEK inhibitor augments antitumor activity of B7-H3-redirected bispecific antibody, Front. Oncol. 10 (2020), https://doi.org/10.3389/fonc.2020.01527.

[36] A. Nagase-Zembutsu, K. Hirotani, M. Yamato, J. Yamaguchi, T. Takata, M. Yoshida, K. Fukuchi, M. Yazawa, S. Takahashi, T. Agatsuma, Development of DS-5573a: a

novel afucosylated mAb directed at B7-H3 with potent antitumor activity, Cancer Sci. 107 (2016) 674–681, https://doi.org/10.1111/cas.12915.

[37] M.J. Goldman, B. Craft, M. Hastie, K. Repečka, F. McDade, A. Kamath, A. Banerjee, Y. Luo, D. Rogers, A.N. Brooks, et al., Visualizing and interpreting cancer genomics data via the Xena platform, Nat. Biotechnol. 38 (2020) 675–678, https://doi.org/10.1038/s41587-020-0546-8.

[38] B.H. Santich, J.A. Park, H. Tran, H.-.F. Guo, M. Huse, N.-K.V. Cheung, Interdomain spacing and spatial configuration drive the potency of IgG-[L]-scFv T cell bispecific antibodies, Sci. Transl. Med. 12 (2020) eaax1315, https://doi.org/10.1126/scitranslmed.aax1315.